Check for updates

Quantifying the trade-off between stiffness and permeability in hydrogels†

Yiwei Gao [ID] and H. Jeremy Cho [ID]*

Hydrogels have a distinct combination of mechanical and water-transport behaviors. As hydrogels stiffen when they de-swell, they become less permeable. Here, we combine de Gennes' semi-dilute polymer theory with the Kozeny-Carman equation to develop a simple, succinct scaling law describing the relationship between mechanical stiffness and hydraulic permeability where permeability scales with stiffness to the −8/9 power. We find a remarkably close agreement between the scaling law and experimental results across four different polymer families with varied crosslinkings. This inverse relationship establishes a fundamental trade-off between permeability and stiffness.

Hydrogels are polymer networks with an interconnected, water-filled porous structure. Water can be absorbed within these pores or permeate through them. The polymer network provides mechanical structure to hydrogels. This leads to hydrogels having a distinct combination of mechanical and water-transport behaviors, making them advantageous for a wide variety of applications. Much of the application-focused studies either study the mechanics in detail (*e.g.*, stimuli-responsive water flow materials, soft robotics, and artificial tissues[1–6]) or transport behavior (*e.g.*, contact lenses, drug delivery, waste-water purification, and solar distillation[7–13]). Currently, there is little understanding of how mechanics and transport behavior could be coupled.

An overarching conclusion from previous studies is that the mesh size in polymer networks dictates the properties of hydrogels.[14] For instance, mesh size controls hydrogel friction, modulus, and permeability.[14–18] One way to control mesh size and thereby change hydrogel properties is to add crosslinking. Naturally, without crosslinking, the polymer network structure has no solid-like rigidity and the polymer solution will flow as a viscous liquid.[19] Crosslinking, by constraining the movement

Department of Mechanical Engineering, University of Nevada, Las Vegas, Las Vegas, NV 89154, USA. E-mail: jeremy.cho@unlv.edu

† Electronic supplementary information (ESI) available. See DOI: https://doi.org/10.1039/d2sm01215d

of polymer strands, adds solid-like elasticity, rendering the hydrogel a viscoelastic material.[20–23] With extremely high cross-linking, the polymer will gain significant brittleness.[24] In our work, we focus on crosslinked hydrogels that behave as solids as we probe their elastic properties at shorter timescales rather than their long-timescale viscous creep behaviors. The feasibility of varying crosslinking density to modify stiffness, permeability, as well as a multitude of other properties has been widely confirmed. Stiffness-focused studies[25–27] have found that higher crosslinking densities generally result in stiffer gels, which is due to a reduced mesh size of the polymer and a denser network structure.[15,16,28,29] Transport-focused studies have found that crosslinking can modify gas or solute permeability[7,30–33] where lower crosslinking densities generally result in higher permeable gels,[34–37] which is due to the enlarged mesh size and enhanced porosity of the network.[14–16] Inspired by the great volume of work establishing the importance of mesh size, we seek to provide a succinct relationship between mechanical stiffness and water permeability of hydrogels as mesh size is varied by crosslinking.

Here, we adopt de Gennes' semi-dilute polymer solution theory[38] as a basis for understanding the influence of mesh size on mechanical stiffness. Previously, we adopted this theory to successfully characterize changes in stiffness, osmotic pressure, and swelling by varying crosslinking density.[27] The semi-dilute theory is a simple, elegant, and experimentally proven description that produces results that are indistinguishable from the more thorough, but complex Flory–Rehner theory that combines Flory–Huggins solution thermodynamics with Gaussian-chain (rubber-like elasticity effects) due to crosslinking.[17,39,40] While the semi-dilute theory does not strictly consider crosslinks, we can assume that the mesh size and corresponding swelling state is set by crosslinking and the osmotic pressure of the environment. The semi-dilute theory provides an illustrative molecular perspective of the most essential part of polymer mixtures, and the properties of polymer networks in a good solvent (like water) are universal and do not depend on how the networks are prepared.[41] With this perspective, the gel is considered to be a solution of

polymer chains that are long and the spacing between the chains, ξ, is what ultimately dictates the properties of the gel. This spacing between polymer chains is related to the polymer volume fraction as

$$\xi = a^{7/4} v^{-1/4} \phi_{\text{poly}}^{-3/4} \qquad (1)$$

where $\phi_{\text{poly}} \equiv V_{\text{poly}}/V$. Equivalently, one can consider this mesh size being related to swelling. If we define the swelling fraction as $s \equiv V/V_{\text{wet}}$ where V_{wet} is the equilibrium volume of a gel in a pure solvent environment, then $\xi \propto s^{3/4}$. For reasons of relating mesh size to porosity, we choose to describe the state of swelling using ϕ_{poly} in this work. Using this scaling result from semi-dilute polymer theory in our previous work[27] where varied ξ by changing crosslinking and the ambient osmotic pressure (*via* changes in humidity), we found that the bulk modulus ultimately depends on the polymer volume fraction—or alternatively the amount of gel swelling, which is inversely proportional to the polymer volume fraction. Thus, from a molecular perspective, changing the crosslinking does not change the stiffness; rather, changing the crosslinking modifies the polymer volume fraction and spacing between polymer chains, which ultimately affects the elastic bulk modulus. This modification of the bulk modulus also equivalently changes the osmotic pressure, $K \sim \Pi$.[27,38] In a semi-dilute system, the precise relationship (des Cloiseaux law) between stiffness, osmotic pressure, and polymer volume fraction is

$$\Pi \sim K = C_I kT \underbrace{a^{-21/4} v^{3/4}}_{\substack{\text{set by} \\ \text{monomer size and} \\ \text{solvent interaction}}} \underbrace{\phi_{\text{poly}}^{9/4}}_{\substack{\text{set by} \\ \text{ambient environment} \\ \text{and crosslinking}}} \qquad (2)$$

with stiffness prefactor label above $a^{-21/4} v^{3/4}$.

where k is the Boltzmann constant, T is absolute temperature, a is the monomer size, and v is the excluded volume of the monomer that depends on the Flory interaction parameter, χ, such that[38]

$$v = a^3 (1 - 2\chi). \qquad (3)$$

Thus, monomers that "dislike" solvent (more positive χ[42]) have smaller effective volumes compared to those that "like" solvent (more negative χ). From eqn (2), we highlight how stiffness scales with polymer volume fraction as $K \propto \phi_{\text{poly}}^{9/4}$, quantifying the effect that gels soften (K decreases) as they swell with water (ϕ_{poly} decreases). We and others previously verified this 9/4 scaling,[27,43–45] validating the semi-dilute description for hydrogels. Furthermore, for pure polyacrylamide gels, we verify this 9/4 scaling through a comparison of mechanical stiffness *versus* polymer mass fraction (Fig. S7a, ESI†).

Inspired by the fact that ϕ_{poly} is an important controlling parameter of gels, we investigate whether ϕ_{poly} also controls the water transport behavior of hydrogels as quantified by the hydraulic permeability. Intuitively, we should expect that by increasing crosslinking, the mesh size, ξ, decreases, causing the polymer volume fraction to increase (decreasing swelling),

and the porosity of the polymer network to decrease. As a result, the polymeric network becomes more constrained, with less porous space.[46–49] Here, we investigate whether this more constrained polymer network increases the difficulty to flow water through it as quantified by the Darcy hydraulic permeability, κ:

$$\kappa = \frac{\mu u}{\nabla P}, \qquad (4)$$

where μ is the dynamic viscosity of water, u is the volumetric flow flux, and ∇P is the hydraulic (pore) pressure gradient.

To test whether higher ϕ_{poly} indeed results in lower permeability, we need a way to independently control ϕ_{poly} without changing other properties of the gel. One way to only change ϕ_{poly} is to alter the osmotic pressure of the environment (*e.g.*, changing the ambient solution environment or humidity). The other way is to vary the crosslinking. We and others have shown that changing crosslinking simply changes ϕ_{poly} (or the equilibrium swelling state) and minimally affects other molecular properties.[27,50] That is, in eqn (2), the monomer size, a, and excluded volume, v, do not change with crosslinker amount—only ϕ_{poly} changes. As such, hydrogels that differ only by crosslinking can be viewed as being a part of the same polymer family. To provide a comprehensive understanding, in this study, we consider 21 different hydrogels spanning across four different polymer families: (1) pure polyacrylamide (PAAm) hydrogels, (2) hydrolyzed PAAm hydrogels,[51,52] (3) PAAm hydrogels with *N,N*-dimethylacrylamide (DMA) as a filler,[53,54] and (4) PAAm hydrogels copolymerized with N-Isopropylacrylamide (PNI-*co*-AAm).[55,56] Within each family, we have five to six different hydrogels differing by crosslinking amount where we use *N,N'*-methylene(bis)acrylamide (MBA) as a crosslinker. The molar crosslinker-to-monomer ratios span 0.5% to 7%. Fourier-transform infrared (FTIR) spectroscopy analysis confirms that significant changes in spectra are observed across different families, but insignificant changes are observed across different crosslinker ratios within the same families (Fig. 2a), consistent with our previous work.[27]

After establishing that crosslinking can be used to independently vary ϕ_{poly}, we test the idea of higher ϕ_{poly} leading to lower hydraulic permeability by performing water transport experiments using a custom-built permeability cell controlled by a microfluidic pressure regulator (Elveflow OB1) and flow rate sensor (see Fig. S1, ESI†). Using Darcy's law (eqn (4)), we find that in the limit of a small pressure difference, ΔP, applied across the gel, the experimentally measurable permeability is

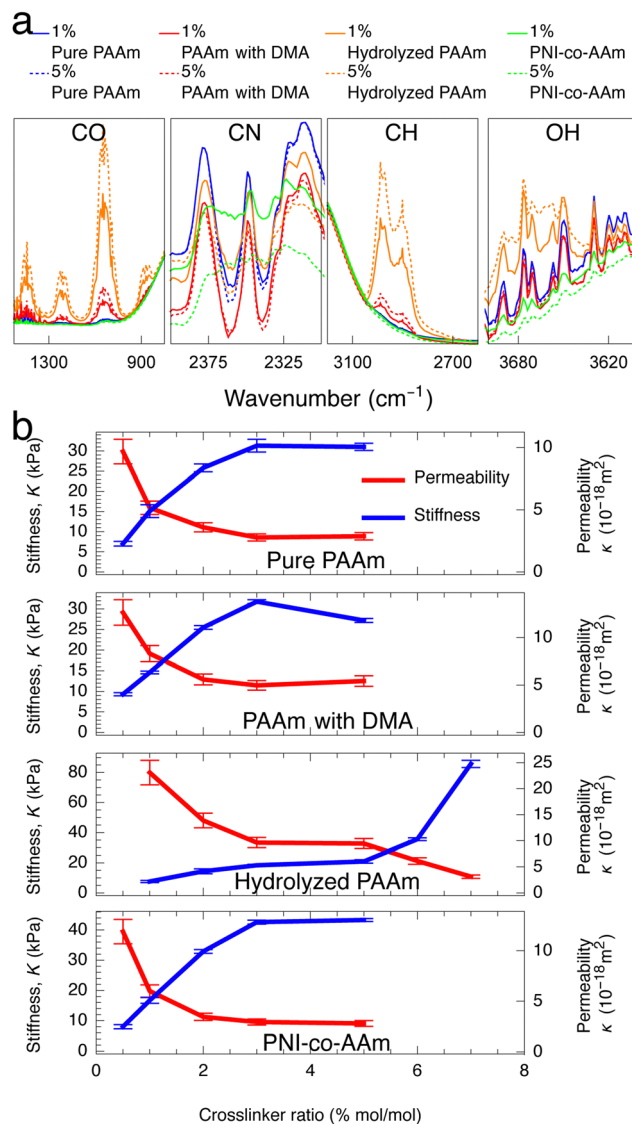$$\kappa \approx \frac{\mu Q L}{A \Delta P} \qquad (5)$$

where Q is the volumetric flow rate, L is the sample thickness, and A is the cross-sectional flow area. Here, we measure Q and control ΔP while μ, A, and L are fixed (L is set to 0.5 mm), measurable constants. If ΔP is appropriately low, then κ would be a constant property and Q would be linear with ΔP. On the other hand, if ΔP is too high, L would decrease due to poroelastic compression of the gel and κ would presumably
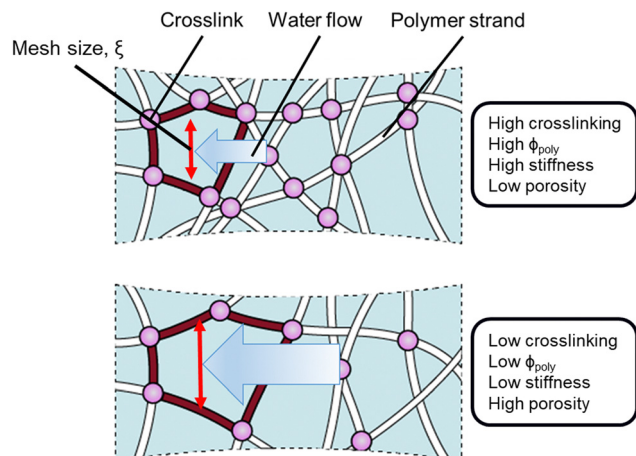
Fig. 1 A scheme of polymeric structure of hydrogels with low and high crosslinking illustrates the differences in mechanical stiffness and water transport. As the crosslinking increases, mesh size, ξ, decreases, the network densifies, resulting in higher stiffness and less porous space, reducing permeability.

Fig. 2 (a) Significant changes in FTIR spectra are only observed across polymer families and not by varied crosslinker ratio. (Complete FTIR test results of all samples are shown in ESI,† Fig. S5) (b) In all four hydrogel families, increasing crosslinker ratio generally increases stiffness and decreases hydraulic permeability with a few polymer-family-specific exceptions. Crosslinker ratios above 5% are not tested for some hydrogels due to high sample brittleness precluding accurate stiffness characterization.

decrease due to densification of the porous network, leading to a nonlinear relationship between Q and ΔP. Informed by previous work on hydrogels under confined loads,[57] the threshold pressure above which these nonlinear effects take hold is related to the bulk modulus of the hydrogel, K. To determine appropriate pressures to test permeability in the linear range, we vary $\Delta P/K$ in the range of 0.1–2 and find that Q is linear with ΔP within $\pm 2\%$ when $\Delta P/K$ is in the range of 0.5–1 (lower pressures introduce measurement uncertainties; see Fig. S2, ESI†). Therefore, to optimize measurement fidelity and minimize poroelastic compression effects, all gels are tested by setting $\Delta P/K = 0.7$.

As expected, the permeability of the tested hydrogels decreases as the crosslinker ratio generally increases from 0.5% to 7% (Fig. 2b, red). However, there are a few notable complications. Increasing crosslinker ratio between 3% to 5% results in very little change (plateau-like trend) or even an increase in permeability (PAAm with DMA). As shown in the hydrolyzed PAAm samples above 5%, the permeability decreases in contrast to the plateau-like behavior at slightly lower crosslinker ratios. Thus, the relationship between permeability and crosslinker ratio is highly polymer-family-specific and would likely need a complicated model to describe accurately. As discussed earlier and in accordance with previous work on mesh size theory,[14–18] polymer volume fraction more directly controls permeability as it does with stiffness. If this were the case, then any changes in permeability should have corresponding inverse changes in stiffness. Therefore, we also measure the stiffness of the tested samples using a custom-built indentation tester (see ESI,† Fig. S3) in accordance with previous testing procedures.[27] Indeed, the stiffness of the hydrogels increases as crosslinker ratio increases (Fig. 2b, blue). Similar to our measurements with permeability, the dependence on crosslinker ratio is highly polymer-family-specific. However, as expected, any changes in permeability

have corresponding inverse changes in stiffness. This coupling between permeability and stiffness is highlighted by the fact that while increasing crosslinker ratio from 3% to 5% for PAAm with DMA results in an anomalous increase in permeability, this is complemented by an anomalous decrease in stiffness. Furthermore, any plateau-like trends in permeability also exist in stiffness. This suggests that both permeability and stiffness are governed by the more fundamental polymer volume fraction and mesh spacing between polymer chains as opposed to the crosslinker ratio (Fig. 1).

If mesh size controls permeability, then we need to incorporate a description of permeability that depends on polymer

volume fraction. Assuming the space between polymer strands, $1 - \phi_{poly}$ is fully wetted by the flowing liquid, then we can define this space as the porosity, ε. This porosity, as confirmed by dissipative particle dynamics simulations,[58] can be related to the permeability. While there are several descriptions relating κ to ε,[18,59] the Kozeny-Carman equation is a simple and widely used model that explicitly defines a relationship between κ and ε and has been used to describe permeability through soft gel materials.[60–63] Here, we take the Kozeny-Carman equation of permeability, substitute $\varepsilon = 1 - \phi_{poly}$, and treat monomer units of the polymer mesh as effective "grains":

$$\kappa = \overbrace{C_{II} \; \Phi_s^2 d^2}^{\substack{\text{permeability prefactor}}} \; \underbrace{\frac{(1 - \phi_{poly})^3}{\phi_{poly}^2}}_{\substack{\text{set by} \\ \text{ambient environment} \\ \text{and crosslinking}}} , \qquad (6)$$

$$\underbrace{\qquad}_{\substack{\text{set by} \\ \text{monomer size} \\ \text{and sphericity}}}$$

where $C_{II} \approx 1/150$ is a constant while Φ_s and d is the sphericity and diameter of monomers, respectively. The monomer diameter, like the excluded monomer volume, ν, should depend on monomer size and solvent interaction with larger diameters associated with more hydrophilic monomers. If we assume these grains are described by the monomer units, then we should not expect Φ_s and d to change significantly with the small amounts of crosslinker nor with the degree of swelling, which is captured by the change in ϕ_{poly}. Rather, the permeability prefactor would likely be determined by the choice, functionalization, or mix of monomer(s) used (polymer family selection).

The swelling-dependent term in the Kozeny-Carman equation can be expanded as $\frac{(1 - \phi_{poly})^3}{\phi_{poly}^2} = \frac{1}{\phi_{poly}^2} - \frac{3}{\phi_{poly}} + 3 - \phi_{poly}$. In the limit of small ϕ_{poly}—applicable to highly swollen gels—the magnitude of the leading-order term, $1/\phi_{poly}^2$, is much greater than the other terms. Thus, for small ϕ_{poly} the permeability can be approximated by the leading-order term as

$$\kappa \approx C_{II} \Phi_s^2 d^2 \phi_{poly}^{-2}. \qquad (7)$$

If this approximation is valid, then the slope of κ using eqn (6) when plotted on a log–log scale should be close to -2 as this is the exponent of the simplified scaling relationship in eqn (7). Indeed, as long as $\phi_{poly} < 0.05$, the difference in values of log–log slope between eqn (6) and (7) is within 8% (see ESI,† Fig. S6). Since, for many swollen hydrogels, ϕ_{poly} is often much smaller than 0.05,[64–67] the relationship in eqn (7) is a very reasonable simplification, providing single-digit-percentage uncertainty or less. Furthermore, for pure PAAm gels, we verify this -2 scaling through a comparison of hydraulic permeability *versus* polymer mass fraction (Fig. S7b, ESI†).

Combining the scaling relationships between stiffness to ϕ_{poly} (eqn (2)) and permeability to ϕ_{poly} (eqn (7)) through the

elimination of ϕ_{poly}, we obtain a scaling law that directly relates stiffness, K, to the hydraulic permeability, κ:

$$\kappa \approx \underbrace{\frac{6^{2/3}(C_I kT)^{8/9} C_{II} \Phi_s^2 (1 - 2\chi)^{4/3}}{\pi^{2/3} a^{2/3}}}_{\substack{\text{prefactor depends on monomer size and solvent interaction} \\ \text{(constant for same polymer family regardless of crosslinking)}}} K^{-8/9} \qquad (8)$$

here, we have used eqn (3) to express the excluded volume, ν in terms of the interaction parameter, χ. This scaling law quantifies the inverse relationship between permeability and stiffness by coupling the semi-dilute polymer description of modulus and the Kozeny-Carman description of hydraulic permeability. This relationship should hold for any hydrogel that varies only by polymer volume fraction, such as if crosslinking were modified. Importantly, the prefactor does not change within the same polymer family: gels with the same monomer size and solvent interaction but different swelling states due to crosslinking. As such, within the same polymer family,

$$\kappa \propto K^{-8/9}. \qquad (9)$$

To verify this simple scaling law, we plot the permeability against the stiffness for the 21 hydrogels across four different polymer families with varied crosslinking from 0.5% to 7% tested earlier on log–log scaling (Fig. 3). In accordance with Eq. 8, each polymer family has data points corresponding to different crosslinker ratios that lie on a slope of $-8/9$. The close agreement within 3.7% uncertainty across a wide range of hydrogel crosslinker ratios provides strong validation of the scaling law (eqn (8)). As mentioned previously, we chose to use the Kozeny-Carman description in accordance with other works involving gels;[60–63] however, we can also generalize the scaling law result (eqn (9)) as $\kappa \propto K^{-4\alpha/9}$ where α scales ϕ_{poly} to κ as $\kappa \propto \phi_{poly}^{-\alpha}$. According to Kapur et al.,[18] α can be the range of 1.4 to 3.3. When explicitly fitting our experimental results to an arbitrary α, we find that $\alpha = 1.8 \pm 0.2$, a result that is within 10% of the Kozeny-Carman exponent of $\alpha = -2$. Nonetheless, we find that setting $\alpha = -2$ (eqn (7)) describes the four tested hydrogel families accurately as we separately verify in Fig. S7b (ESI†),
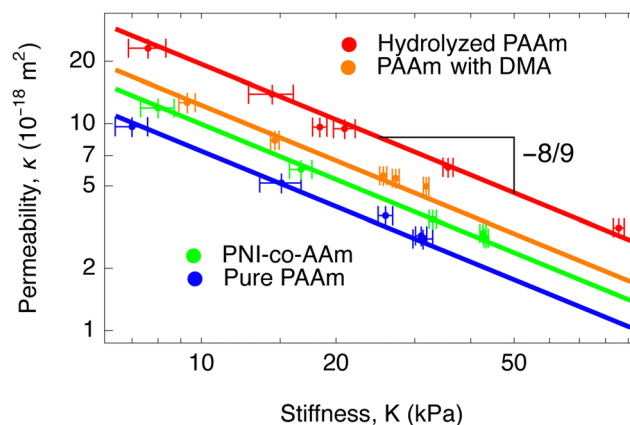

Fig. 3 Plotting permeability and stiffness of 21 hydrogels with varying crosslinker ratio across four polymer families shows a close agreement with eqn (8) where the log–log slope is $-8/9$.

thereby validating the Kozeny-Carman description for hydrogels. We highlight the fact that for hydrolyzed PAAm gels, we are able to obtain more than a decade range of stiffness and find that the scaling still holds. Thus, the scaling law allows one to determine the permeability of gels based on its stiffness as long as the prefactor in eqn (8) has been determined from a reference sample in the same polymer family. Interestingly, the prefactor in eqn (8) suggests that monomers that are rendered more hydrophilic (decreasing χ), κ should increase. This is in agreement with our results where the more hydrophilic hydrolyzed PAAm (Fig. 3, red) has a higher permeability than its more hydrophobic pure PAAm counterpart (Fig. 3, blue) at the same stiffness.

In conclusion, our work confirms that combining de Gennes' semi-dilute polymer theory and the Kozeny-Carman equation provides an accurate scaling law relating permeability to the stiffness of hydrogels. Our resulting scaling law between permeability and stiffness (1) reconfirms the importance mesh size (and therefore, degree of swelling and polymer volume fraction) on hydrogel properties, and (2) provides a simple, succinct, and experimentally testable relationship between mechanical stiffness and water permeability of hydrogels. Future studies could investigate whether the scaling law can be applied to hydrogels with high entanglement[68,69] or sliding crosslinkers[70–72] to alter polymer volume fraction. Future studies could also investigate the validity of the scaling law for gas permeability or liquid solution permeabilities where polymer volume fraction is modified through osmotic pressure rather than crosslinking. We anticipate that our work will guide the informed synthesis of hydrogels tuned by crosslinker amount for applications in a wide variety of fields.

Author contributions

Y. G. performed data curation, investigation, methodology, and validation. H. J. C. performed supervision and project administration. Both Y. G. and H. J. C. performed conceptualization, formal analysis, visualization, and writing.

Conflicts of interest

There are no conflicts to declare.

Acknowledgements

Notes and references

1 H.-L. Tan, S.-Y. Teow and J. Pushpamalar, *Bioengineering*, 2019, **6**, 17.

2 Y. Zhou, C. Wan, Y. Yang, H. Yang, S. Wang, Z. Dai, K. Ji, H. Jiang, X. Chen and Y. Long, *Adv. Funct. Mater.*, 2019, **29**, 1806220.

3 R. Subramani, A. Izquierdo-Alvarez, P. Bhattacharya, M. Meerts, P. Moldenaers, H. Ramon and H. Van Oosterwyck, *Front. Mater.*, 2020, **7**, 212.

4 K. Liu, Y. Zhang, H. Cao, H. Liu, Y. Geng, W. Yuan, J. Zhou, Z. L. Wu, G. Shan and Y. Bao, *et al.*, *Adv. Mater.*, 2020, **32**, 2001693.

5 S. Lin, H. Yuk, T. Zhang, G. A. Parada, H. Koo, C. Yu and X. Zhao, *Adv. Mater.*, 2016, **28**, 4497–4505.

6 S. Jiang, S. Liu and W. Feng, *J. Mech. Behav. Biomed. Mater.*, 2011, **4**, 1228–1233.

7 N. Efron, P. B. Morgan, I. D. Cameron, N. A. Brennan and M. Goodwin, *Optom. Vis. Sci.*, 2007, **84**, E328–E337.

8 J. Kim, A. Conway and A. Chauhan, *Biomaterials*, 2008, **29**, 2259–2269.

9 L. Zhao, P. Wang, J. Tian, J. Wang, L. Li, L. Xu, Y. Wang, X. Fei and Y. Li, *Sci. Total Environ.*, 2019, **668**, 153–160.

10 V. Sinha and S. Chakma, *J. Environ. Chem. Eng.*, 2019, **7**, 103295.

11 H. Lu, W. Shi, F. Zhao, W. Zhang, P. Zhang, C. Zhao and G. Yu, *Adv. Funct. Mater.*, 2021, **31**, 2101036.

12 V. Van Tran, D. Park and Y.-C. Lee, *Environ. Sci. Pollut. Res.*, 2018, **25**, 24569–24599.

13 D. S. Jones, C. P. Lorimer, C. P. McCoy and S. P. Gorman, *J. Biomed. Mater. Res., Part B*, 2008, **85**, 417–426.

14 N. R. Richbourg and N. A. Peppas, *Prog. Polym. Sci.*, 2020, **105**, 101243.

15 Y. Gombert, R. Simič, F. Roncoroni, M. Dübner, T. Geue and N. D. Spencer, *Adv. Mater. Interfaces*, 2019, **6**, 1901320.

16 A. A. Pitenis and W. G. Sawyer, *Tribol. Lett.*, 2018, **66**, 1–7.

17 S. P. Obukhov, M. Rubinstein and R. H. Colby, *Macromolecules*, 1994, **27**, 3191–3198.

18 V. Kapur, J. C. Charkoudian, S. B. Kessler and J. L. Anderson, *Ind. Eng. Chem. Res.*, 1996, **35**, 3179–3185.

19 M. Huang, H. Furukawa, Y. Tanaka, T. Nakajima, Y. Osada and J. P. Gong, *Macromolecules*, 2007, **40**, 6658–6664.

20 L. Cacopardo, N. Guazzelli, R. Nossa, G. Mattei and A. Ahluwalia, *J. Mech. Behav. Biomed. Mater.*, 2019, **89**, 162–167.

21 T. L. Sun, T. Kurokawa, S. Kuroda, A. B. Ihsan, T. Akasaki, K. Sato, M. Haque, T. Nakajima and J. P. Gong, *et al.*, *Nat. Mater.*, 2013, **12**, 932–937.

22 O. Chaudhuri, *Biomater. Sci.*, 2017, **5**, 1480–1490.

23 D. Huang, Y. Huang, Y. Xiao, X. Yang, H. Lin, G. Feng, X. Zhu and X. Zhang, *Acta Biomater.*, 2019, **97**, 74–92.

24 Y. Kawauchi, Y. Tanaka, H. Furukawa, T. Kurokawa, T. Nakajima, Y. Osada and J. P. Gong, *J. Phys.: Conf. Ser.*, 2009, 012016.

25 S. Lin and L. Gu, *Materials*, 2015, **8**, 551–560.

26 S. P. Pilipchuk, M. K. Vaicik, J. C. Larson, E. Gazyakan, M.-H. Cheng and E. M. Brey, *J. Biomed. Mater. Res., Part A*, 2013, **101**, 2883–2895.

27 Y. Gao, N. K. Chai, N. Garakani, S. S. Datta and H. J. Cho, *Soft Matter*, 2021, **17**, 9893–9900.

28 Y. Tanaka, M. Seii, J. Sui and M. Doi, *J. Chem. Phys.*, 2020, **152**, 184901.

29 H. J. Kwon, A. Kakugo, T. Ura, T. Okajima, Y. Tanaka, H. Furukawa, Y. Osada and J. P. Gong, *Langmuir*, 2007, **23**, 6257–6262.

30 H. Ju, A. C. Sagle, B. D. Freeman, J. I. Mardel and A. J. Hill, *J. Membr. Sci.*, 2010, **358**, 131–141.

31 C.-C. Peng and A. Chauhan, *J. Membr. Sci.*, 2012, **399**, 95–105.

32 J. Pozuelo, V. Compañ, J. M. González-Méijome, M. González and S. Mollá, *J. Membr. Sci.*, 2014, **452**, 62–72.

33 L. Liu, A. Chakma and X. Feng, *J. Membr. Sci.*, 2008, **310**, 66–75.

34 H. Matsuyama, M. Teramoto and H. Urano, *J. Membr. Sci.*, 1997, **126**, 151–160.

35 M. K. Yazdi, V. Vatanpour, A. Taghizadeh, M. Taghizadeh, M. R. Ganjali, M. T. Munir, S. Habibzadeh, M. R. Saeb and M. Ghaedi, *Mater. Sci. Eng., C*, 2020, **114**, 111023.

36 A. C. Sagle, H. Ju, B. D. Freeman and M. M. Sharma, *Polymer*, 2009, **50**, 756–766.

37 M. J. Tavera-Quiroz, J. J. F. Daz and A. Pinotti, *Int. J. Appl. Eng. Res.*, 2018, **13**, 13302–13307.

38 P.-G. De Gennes, *Scaling concepts in polymer physics*, Cornell university press, 1979.

39 R. van der Sman, *Food Hydrocolloids*, 2015, **48**, 94–101.

40 A. Fernandez-Nieves, H. Wyss, J. Mattsson and D. A. Weitz, *Microgel suspensions: fundamentals and applications*, John Wiley & Sons, 2011.

41 S. Panyukov, *Sov. Phys. JETP*, 1990, **71**, 372–379.

42 E. Nagy, *Basic Equations of Mass Transport through a Membrane Layer*, 2019, vol. 2, pp. 457–481.

43 M. Zrinyi and F. Horkay, *Polymer*, 1987, **28**, 1139–1143.

44 S. P. Obukhov, M. Rubinstein and R. H. Colby, *Macromolecules*, 1994, **27**, 3191–3198.

45 C. L. Bell and N. A. Peppas, *Biopolymers II*, Berlin, Heidelberg, 1995, pp. 125–175.

46 R. da Silva and M. G. de Oliveira, *Polymer*, 2007, **48**, 4114–4122.

47 N. E. Ben Ammar, T. Saied, M. Barbouche, F. Hosni, A. H. Hamzaoui and M. Şen, *Polym. Bull.*, 2018, **75**, 3825–3841.

48 M. N. Collins and C. Birkinshaw, *J. Appl. Polym. Sci.*, 2011, **120**, 1040–1049.

49 S. J. Bryant, K. S. Anseth, D. A. Lee and D. L. Bader, *J. Orthop. Res.*, 2004, **22**, 1143–1149.

50 J. Li, Y. Hu, J. J. Vlassak and Z. Suo, *Soft Matter*, 2012, **8**, 8121–8128.

51 S. Saber-Samandari, M. Gazi and E. Yilmaz, *Polym. Bull.*, 2012, **68**, 1623–1639.

52 J. Aalaie and A. Rahmatpour, *J. Macromol. Sci., Part B: Phys.*, 2007, **47**, 98–108.

53 S. Skelton, M. Bostwick, K. O'Connor, S. Konst, S. Casey and B. P. Lee, *Soft Matter*, 2013, **9**, 3825–3833.

54 E. A. Kuru, N. Orakdogen and O. Okay, *Eur. Polym. J.*, 2007, **43**, 2913–2921.

55 B. Manjula, K. Varaprasad, R. Sadiku and K. M. Raju, *Adv. Polym. Technol.*, 2013, **32**(2), 21340.

56 L. Yang, X. Fan, J. Zhang and J. Ju, *Polymers*, 2020, **12**, 389.

57 J.-F. Louf, N. B. Lu, M. G. O'Connell, H. J. Cho and S. S. Datta, *Sci. Adv.*, 2021, **7**, eabd2711.

58 B. Hertzberg, A. Alexeev and G. Yushin, *J. Am. Chem. Soc.*, 2010, **132**, 8548–8549.

59 L. Spielman and S. L. Goren, *Environ. Sci. Technol.*, 1968, **2**, 279–287.

60 S.-I. Nakao, T. Nomura and S. Kimura, *AIChE J.*, 1979, **25**, 615–622.

61 S. Zaidi and A. Kumar, *Desalination*, 2005, **172**, 107–117.

62 E. Iritani, N. Katagiri, K. Yamaguchi and J.-H. Cho, *Drying Technol.*, 2006, **24**, 1243–1249.

63 N. Isobe, S. Kimura, M. Wada and S. Deguchi, *J. Taiwan Inst. Chem. Eng.*, 2018, **92**, 118–122.

64 W. Zhang, Y. Liu, M. Zhu, Y. Zhang, X. Liu, H. Yu, Y. Jiang, Y. Chen, D. Kuckling and H.-J. P. Adler, *J. Polym. Sci., Part A: Polym. Chem.*, 2006, **44**, 6640–6645.

65 Q. Lv, M. Wu and Y. Shen, *Colloids Surf., A*, 2019, **583**, 123972.

66 S. J. Kim, S. J. Park and S. I. Kim, *React. Funct. Polym.*, 2003, **55**, 53–59.

67 A. Kumar, M. Pandey, M. Koshy and S. A. Saraf, *Int. J. Drug Delivery*, 2010, **2**, 135–140.

68 J. Kim, G. Zhang, M. Shi and Z. Suo, *Science*, 2021, **374**, 212–216.

69 K. Chen, Y. Feng, Y. Zhang, L. Yu, X. Hao, F. Shao, Z. Dou, C. An, Z. Zhuang and Y. Luo, *et al.*, *ACS Appl. Mater. Interfaces*, 2019, **11**, 36458–36468.

70 J. P. Gong, *Soft Matter*, 2010, **6**, 2583–2590.

71 R. Du, Z. Xu, C. Zhu, Y. Jiang, H. Yan, H.-C. Wu, O. Vardoulis, Y. Cai, X. Zhu and Z. Bao, *et al.*, *Adv. Funct. Mater.*, 2020, **30**, 1907139.

72 C.-Y. Shi, Q. Zhang, C.-Y. Yu, S.-J. Rao, S. Yang, H. Tian and D.-H. Qu, *Adv. Mater.*, 2020, **32**, 2000345.